Energy Commission through Contract No. W-31-109-Eng-38.

## NOTATION

$a$ = dimensionless age, random variable
$D_p$ = particle diameter
$E\{\ \}$ = expected value
$f$ = residence time density function
$F$ = residence time distribution function
$F\{\ \}$ = Fourier transform
$K+1$ = number of equally spaced observations
$n$ = lowest number for which $Z_n \rightarrow 0$
$N$ = total number of particles observed
$N_{Nu}$ = transport coefficient
$\overline{N}_{Nu}$ = average transport coefficient
$N_{Nu}(a)$ = instantaneous transport coefficient
$N(t)$ = number of elements in residence at time $t$, random function
$P_N$ = probability mass function
$R$ = autocorrelation function
$S$ = spectral density function
$t$ = time
$v$ = superficial gas velocity
$v_{mf}$ = superficial gas velocity at minimum fluidization
$W$ = weighting function
$W(j\Delta t)$ = weight function in estimator for spectral density
$X_0$ = estimator for $\overline{N}$
$Y_j$ = estimator for $\psi(j\Delta t)$
$Z_j$ = modified estimator for $\psi(j\Delta t)$

### Greek Letters

$\alpha$ = shape factor for gamma distribution
$\Delta t$ = time difference between observations
$\theta$ = dimensional residence time
$\overline{\theta}$ = $E\{\theta\}$
$\sigma\{\ \}$ = standard deviation
$\sigma^2\{\ \}$ = variance
$\tau$ = dimensionless residence time, random variance
$\overline{\tau}$ = $E\{\tau\}$
$\phi$ = age density function
$\psi$ = autocovariance function
$\omega$ = frequency
$\omega_N$ = Nyquist frequency

### Superscripts

$-$ = mean value over distribution
$\wedge$ = estimate

## LITERATURE CITED


1. Abramowitz, M., and I. A. Stegun, "Handbook of Mathematical Functions with Formulas, Graphs, and Mathematical Tables," Natl. Bur. Stds., App. Math. Ser. 55, 4th printing (Dec., 1965).
2. Blackman, R. B., and J. W. Tukey, "The Measurement of Power Spectra from the Point of View of Communication Engineering," Dover, New York (1958).
3. Davis, P. J., and R. Rabinowitz, "Numerical Integration," Blaidsell, Mass. (1967).
4. Grenander, U., and M. Rosenblatt, "Statistical Analysis of Stationary Time Series," Wiley, New York (1957).
5. Jenkins, G. M., *Technometrics*, 3, No. 2, 133-166 (1961).
6. Koppel, L. B., "Statistical Models for Surface Renewal in Heat and Mass Transfer: Part V, Maximum and Minimum Transport Coefficients."
7. ———, R. D. Patel, and J. T. Holmes, *AIChE J.*, **12**, 947-955 (1966).
8. Patel, R. D., Ph.D. thesis, Purdue Univ., Lafayette, Ind. (1967).
9. ———, *ANL-7353*, Argonne National Laboratory, Argonne, Ill.
10. ———, L. B. Koppel, and J. T. Holmes, *AIChE J.*
11. Solodovnikov, V. V., "Introduction to the Statistical Dynamics of Automatic Control Systems," Dover, New York (1960).
12. Wilks, S. S., "Mathematical Statistics," Wiley, New York (1962).


# Part IV: Wall to Fluidized Bed Heat Transfer Coefficients

**Heat transfer coefficients were measured for glass particles at the same wall surface of a fluidized bed for which glass particle residence times were measured in a previous study. The data compared well with theoretical predictions of the dependence of heat transfer coefficients on particle residence times. Heat transfer coefficients for metal particle systems, for which direct measurements of residence times were not available, were predicted with fair accuracy by estimating residence times from a dimensionless correlation proposed in a previous study. The ability of the particle surface renewal models to accurately predict heat transfer coefficients is strong evidence of their physical validity.**

## DISCUSSION OF PREVIOUS WORK

Current information strongly suggests that heat transfer from a surface to a gas fluidized bed is a surface renewal transport process. Several authors have proposed surface renewal models for predicting wall to fluidized bed heat transfer coefficients. Mickley and Fairbanks (*9*) envisage clumps of particles, or packets, arriving at the heated surface, receiving heat by unsteady state transfer, and returning to the bulk of the bed. The packets have the properties of the bed at minimum fluidization conditions. The heat transfer coefficient is shown to be proportional to a stirring factor and to the square root of the packet thermal conductivity, specific heat, and density. The stirring factor depends on the frequency of renewal of the packets at the heated surface and is assumed to include the effect of particle diameter. The deficiencies in this model are that the heat transfer coefficient is directly proportional to the square root of particle heat capacity, which is unrealistic, as pointed out by Ziegler et al. (*15*); and the predicted heat transfer coefficient is inversely proportional to the square root of the mean age of the packets, so that at zero age the predicted coefficient is infinite, whereas at infinite age (corresponding to minimum fluidization conditions) it is zero.

Baskakov (*2*) proposed a similar model with an added contact resistance to heat transfer located at the wall-facing surfaces of the particles which are in contact with the wall. Because of the contact resistance, the heat transfer coefficient for zero age does not become infinite but is determined by the finite contact resistance at the wall. However, for infinitely large values of the age, the coefficient goes to zero, which is a theoretical deficiency.

Ziegler, Koppel, and Brazelton (*15*) have proposed a

model similar to Mickley's. Instead of considering the packets, these authors consider the heating of a cold sphere surrounded by a stagnant gas at the hot wall temperature and obtain a time averaged heat transfer coefficient by assuming a residence time distribution of the gamma form. Their model is also deficient at infinite age.

Botterill et al. (*4, 5*) have considered the transient heating of spheres at a hot wall. They calculated the variation in the heat flux with age of a sphere by numerical solution of the energy equation for the gas-sphere system. The average heat flux was found and compared with experimental data obtained in a scraped surface fluidized bed. (A set of stirring blades served to sweep particles away from the hot wall at a fixed frequency; an artificial residence time was thus imposed on the particles.) There was good agreement with the theoretical predictions.

Although the residence times of particles are of fundamental importance to these surface renewal models, few attempts have been made to either measure them experimentally or to predict them theoretically. Mickley, Fairbanks, and Hawthorn (*10*) indirectly determined the renewal frequency of packets of particles at the surface of a low heat capacity heater in a fluidized bed by measuring the temperature fluctuations of the heater. They then used these renewal frequencies in combination with their heat transfer model (*9*) to arrive at good predictions of the time average heat transfer coefficient. Ruckenstein (*13*) used instability theory to predict the renewal frequency as defined by Mickley et al. (*10*) and showed that the renewal frequency is a weak function of the velocity of fluidization, as was also found experimentally by Mickley (*10*). Apart from these indirect evaluations of particle residence times, no reference in the literature can be found wherein the particle residence times were measured directly.

The present work develops models which eliminate some of the undesirable characteristics of previous models, namely, the prediction of an infinite coefficient at zero residence time and/or zero coefficient at infinite residence time. The models are tested by comparison with experimental data, direct measurements of heat transfer coefficients and particle residence times at the same wall surface.

## EXPERIMENTAL TECHNIQUE

A detailed description of the experimental equipment and measurement techniques has been given by Patel (*11*).

Overall heat transfer coefficients were measured from a 1½ in. wide by 2 in. high section of the fluidized bed wall located approximately 5 in. above the distributor plate in the 4.5 in. diameter column. The heater was of adiabatic design (the main heater being surrounded by guard heaters) ensuring that practically all electrical power supplied to it was transferred as heat to the bed only. Electrical power to the main heater was measured by a calibrated ammeter and voltmeter; this power divided by the heater surface area gave the wall heat flux $q$. Three thermocouples located at the surface of the main heater served to measure its temperature $t_w$. The bed temperature $t_b$ was measured at two positions and the average taken. Bed temperatures were virtually the same at different locations sufficiently far from the heater. The heat transfer coefficient was then calculated as $h = q/(t_w - t_b)$.

Gas bubbles were eliminated by stirring the bed just below the heater with a paddle type of stirrer at approximately 400 rev./min. Transport at the bubble free surface can be analyzed by surface renewal models without consideration of the complex effects of bubbles; thus, a source of confusion is eliminated. The methods used to measure residence times have been discussed elsewhere (*8, 12*). These residence time measurements were made at the identical surface, a transparent plate being used in place of the adiabatic heater. The experimental measurements thus provided heat transfer coefficients and residence times at the same wall surface under identical conditions of fluidization.

Eight types of particles were used in the heat transfer studies. Their properties are given in Table 1. Residence times were measured for the glass particles only, since a convenient black and white tagging was available (*11*). Residence times for the other systems were not measured but were estimated from a dimensionless correlation of the residence time measurements obtained for the glass particles and for cellulose acetate particles, as described in Part III (*12*). No convenient tagging method has been developed for the copper, alumina, and aluminum particles. Heat transfer coefficients were measured for all eight particle types.

The maximum error in the measured heat transfer coefficients is estimated to be 10%. The combined error due to errors in both heat transfer coefficients and average residence times is about 12% (*11*). This latter figure is appropriate for comparisons between experiment and theory, such as those presented in Figures 3 to 5.

## THEORY

Two film penetration type of models for wall to bed heat transfer are developed below. Model I considers transient heat transfer to a packet of particles at the wall, assuming a nonzero wall to packet thermal resistance. Model II considers the transient heating of a particle at the wall, the particle gaining heat by convection from the surrounding fluid and losing heat to a packet of particles behind it. In both models, the packet is assumed to be of finite thickness, thus yielding film penetration type of mechanisms [Toor and Marchello (*14*)].

### MODEL I

The geometry of this model is shown in Figure 1. The following assumptions are made:

1. A packet of particles initially at temperature $t_b$, the bulk bed temperature, arrives at the wall surface (temperature $t_w$) at time zero. The packet of particles is assumed to possess the properties of the bed at minimum fluidization conditions [as in Mickley (*9*)].
2. The packet receives heat from the wall and then returns to the bed. Heat flows from the wall to the packet across a contact resistance $1/h_c$.
3. The packet possesses a characteristic thickness $L$, beyond which distance the temperature is constant at $t_b$.
4. Thermal properties of the gas and particles are constant.
5. Heat transfer from wall to packet by radiation is negligible (*1*).

Under these assumptions, the differential equation and boundary conditions for the system may be written in dimensionless form as

$$\frac{\partial T_m}{\partial a} = \frac{\partial^2 T_m}{\partial x^2} \tag{1}$$

$$T_m(x, 0) = 0 \tag{2}$$

$$T_m\left(\frac{L}{D_p}, a\right) = 0 \tag{3}$$

$$\frac{\partial T_m}{\partial x}(0, a) = M[T_m(0, a) - 1] \tag{4}$$

where

$$T_m(x, a) = \frac{t_m(y, \theta) - t_b}{t_w - t_b} \qquad a = \frac{\theta \alpha_m}{D_p^2}$$

$$x = \frac{y}{D_p} \qquad M = \frac{h_c D_p}{k_m} \tag{4a}$$

Table 1. Properties of Fluidized Particles

| Particle type | Wt. mean particle diam., ft. $\times 10^3$ | Min. fluidized vel. (superficial), ft./min. | Void fraction at min. fluidization | Solid density, lb./cu. ft. | Solid thermal conductivity, B.t.u./(hr.)(ft.)(°F.) | Solid specific heat, B.t.u./(lb.)(°F.) |
|---|---|---|---|---|---|---|
| No. 1 glass | 2.65 | 83.5 | 0.40 | 154 | 0.5 | 0.17 |
| No. 2 glass | 1.94 | 50.8 | 0.41 | 154 | 0.5 | 0.17 |
| No. 3 glass | 1.03 | 19.0 | 0.41 | 154 | 0.5 | 0.17 |
| No. 1 copper | 2.00 | 145.0 | 0.40 | 557 | 222.0 | 0.10 |
| No. 2 copper | 1.05 | 57.22 | 0.41 | 557 | 222.0 | 0.10 |
| No. 1 alumina | 1.98 | 109.0 | 0.55 | 250 | 19.0 | 0.193 |
| No. 2 alumina | 0.99 | 31.5 | 0.54 | 250 | 19.0 | 0.193 |
| Aluminum | 0.98 | 19.7 | 0.44 | 169 | 117.5 | 0.224 |

This system of equations is similar to the formulation of the film penetration model first presented by Toor and Marchello (*14*). It becomes identical to that of Toor and Marchello (*14*) if Equation (4) is replaced by

$$T_m(0, a) = 1 \tag{5}$$

or, what is equivalent, if the contact Nusselt number $M$ in Equation (4) is infinite. It becomes identical to Baskakov's (*2*) system if Equation (3) is replaced by

$$T_m(\infty, a) = 0 \tag{6}$$

It becomes identical to Mickley's (9) system if in addition to replacing Equation (3) by (6) we further replace Equation (4) by (5). The model is thus a film penetration model with a contact resistance at the transporting surface.

The solution of the system of Equations (1) to (4) is well known and is given by Carslaw and Jaeger (*6*). The solution for the instantaneous and average Nusselt numbers is of more interest.

#### Instantaneous Nusselt Number

Defining an overall instantaneous heat transfer coefficient by

$$h(a) = \frac{q(a)}{t_w - t_b} \tag{7}$$

and the instantaneous Nusselt number by

$$N_{Nu}(a) = \frac{h(a)D_p}{k_m} \tag{8}$$

and using the Laplace transform, we obtain for the Laplace transform of the instantaneous Nusselt number:

$$N_{Nu}(p) = \frac{M}{\sqrt{p}\left(\sqrt{p} + M \tanh \dfrac{L\sqrt{p}}{D_p}\right)} \tag{9}$$

#### Average Nusselt Number

In general, the instantaneous Nusselt number is of less interest than the average Nusselt number. The average Nusselt number $\overline{N}_{Nu}$ is defined in terms of a surface-age density function $\phi(a)$ as

$$\overline{N}_{Nu} = \int_0^\infty N_{Nu}(a)\ \phi(a)\ da \tag{10}$$

In this form, the average Nusselt number may be difficult to evaluate, depending on the form of $\phi(a)$. However, for special forms of $\phi(a)$, one of which is the exponential form, Koppel et al. (7) have derived operational techniques for arriving at the average Nusselt number using the Laplace transform of the instantaneous Nusselt number. The age density function $\phi(a)$ is related to the residence time density function and may be calculated from it by using Equation (1) of Part I (7).

In Part V, it will be shown that the use of an exponential residence time density having the observed mean value $\bar{\tau}$ does not introduce significant error into the value computed for $\overline{N}_{Nu}$. In other words, if the average residence time is held fixed, changing the shape of the residence time density curve does not significantly change $\overline{N}_{Nu}$. A qualitative indication of this result was also given in Part I. Therefore, we henceforth use

$$\phi(a) = \frac{1}{\bar{\tau}} \exp(-a/\bar{\tau}); \quad a > 0 \tag{11}$$

to compute $\overline{N}_{Nu}$. Use of Equation (11) of Part I on Equation (9) yields, after minor rearrangements

$$\eta_1(\zeta_1; \xi_1) = \frac{1}{1 + \zeta_1 \tanh(\xi_1/\zeta_1)} \tag{12}$$

where

$$\eta_1 = \frac{\overline{N}_{Nu}}{M}$$

$$\zeta_1 = M\sqrt{\bar{\tau}} \tag{13}$$

$$\xi_1 = ML/D_p$$

This is the basic result of model I.

#### Asymptotic Values

Some limiting forms of this equation will be useful in the sequel. The dimensionless contact coefficient is defined as the instantaneous Nusselt number at zero age. Clearly, if $\bar{\tau} \to 0$, then $\overline{N}_{Nu} \to N_{Nu}(0)$, so the contact coefficient can be obtained from Equation (12) as

$$\eta_1(0; \xi_1) = 1 \tag{14}$$

This result is obvious; however, the approach will be useful for defining a contact resistance for model II. Conversely, as $\bar{\tau} \to \infty$, then $\overline{N}_{Nu} \to N_{Nu}(\infty)$, and we obtain from Equation (12) an expression for $N_{Nu}(\infty)$:

$$\eta_1(\infty; \xi_1) = \frac{1}{1 + \xi_1} \tag{15}$$

Clearly, the condition of incipient fluidization corresponds to $\zeta_1 = \infty$. Therefore, Equations (14) and (15) will be useful for calculating the parameter $\xi_1$ from the observed value of $h_{mf}$, the heat transfer coefficient at incipient fluidization. Equations (14) and (15) show that model I pre-

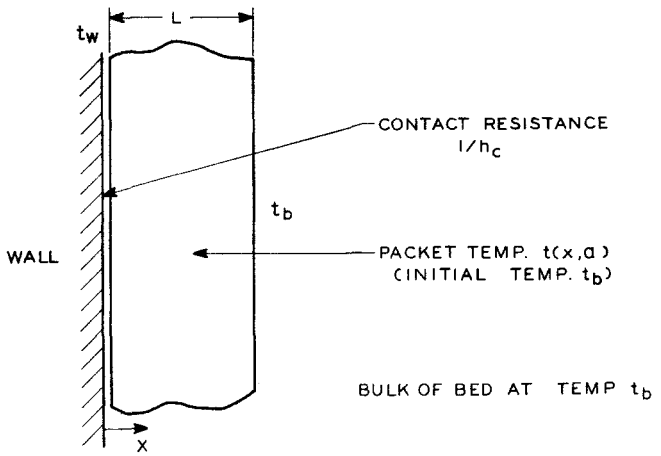


Fig. 1. Geometry for model I.

dicts finite heat transfer at high velocity ($\bar{\tau} \to 0$) and nonzero heat transfer at stagnant conditions ($\bar{\tau} \to \infty$), as observed in physical systems.

If $L/D_p \to \infty$ and hence $\xi_1 \to \infty$, Equation (15) yields a zero transport coefficient as $\bar{\tau} \to \infty$. The result is the pure penetration form of model I, which is originally a film penetration model. Operating on Equation (12), we obtain its pure penetration asymptote:

$$\eta_1(\zeta_1; \infty) = \frac{1}{1 + \zeta_1} \tag{16}$$

This result corresponds to the model of Baskakov (*2*), since it contains a contact resistance but no film mechanism.

If, also, $M \to \infty$, Equation (14) yields an infinite heat transfer coefficient as $\bar{\tau} \to 0$. The result is the zero contact resistance form of the pure penetration model in Equation (16). Operating on Equation (16), we obtain this form as

$$\lim_{M \to \infty} \eta_1(\zeta_1; \infty) = \frac{1}{\zeta_1} \tag{17}$$

This result is almost identical to the model of Mickley (*9*), who used an impulse form of the residence time density to obtain Equation (17) multiplied by the factor $2/\sqrt{\pi}$, which is essentially unity.

Returning to Equation (12), if $M \to \infty$, we obtain the zero contact resistance form of model I. Operating on Equation (12), we get

$$\lim_{M \to \infty} \eta_1(\zeta_1; \xi_1) = \frac{1}{\zeta_1 \tanh(\xi_1/\zeta_1)} \tag{18}$$

This is the film penetration model of transport without a contact resistance and corresponds to the model of Toor and Marchello (*14*).

#### General Transport Phenomena

For application to transport phenomena other than fluidized bed heat transfer, it is necessary to define dimensionless quantities by using $L$ in place of $D_p$. Denote these redefined quantities by asterisks (for example, $\overline{N}_{Nu}{}^* = \overline{h}L/k_m$, $\bar{\tau}^* = \bar{\theta}\alpha_m/L^2$, $\eta_1{}^* = N_{Nu}{}^*/M^*$, $\xi_1{}^* = M^* = h_cL/k_m$, $\zeta_1{}^* = \zeta_1$, etc.). Then the film penetration model with contact resistance becomes identical to Equation (12) but with asterisks on all quantities. Similarly, the asymptotic values and special cases in Equations (14) to (18) are converted to this basis by placing asterisks on all quantities. Of particular interest is the result obtained in this manner from Equation (18), which rearranges to

$$\overline{N}_{Nu}{}^* = \frac{1}{\sqrt{\bar{\tau}^*} \tanh\left(\frac{1}{\sqrt{\bar{\tau}^*}}\right)} \tag{19}$$

This is the basic result of Toor and Marchello (*14*) in closed form. These authors give two infinite series (for short and long average residence times, respectively) for the average Nusselt number and use only the first term in each to approximate $\overline{N}_{Nu}$. As shown by Patel (*11*), both of their series may be summed to give Equation (19).

#### Application to Fluidized Bed Heat Transfer

Baskakov (*2*) has presented a relation for $h_c$ by considering temperature gradients in a particle in contact with a hot wall. He postulates that temperature gradients exist in the particle only up to a depth $d$ times the particle radius, $d$ being fractional, and by considering the thermal resistance due to the gas and to this postulated layer in the particle, he obtains

$$M = \frac{\pi k_g}{k_m}\left[\ln\left(\frac{k_s}{dk_g}\right) - 1\right] \tag{20}$$

Note that $M$ is not sensitive to the value of $d$, for which Baskakov recommends the value of 0.1. Use of this value of $M$ and the observed value of $h_{mf}$ in Equation (15) yields the value of $\xi_1$.

In practice, the mean residence times of packets at the surface is difficult to determine. It is possible to measure residence times of particles at the surface by tracer techniques (*8, 10*). During the present work it was observed that particles tended to move in groups downwards along the wall, with only a few particles (less than 5%) moving away from or towards the wall in a radial direction. Such downward motion is typical of particles at fluidized bed walls. This would imply that the particles are representative of the packets and that particle residence times are virtually the same as packet residence times. Since some particles do move away from and towards the surface radially, one should expect that particle residence times are in general slightly shorter than packet residence times.

### MODEL II

The geometry of this model is shown in Figure 2. The following assumptions are made:

1. The fluidized particles are spheres of uniform diameter $D_p$.
2. Particles at temperature $t_b$ from the bulk of the fluidized bed arrive at the heating surface which is at temperature $t_w$, receive heat by convection from the approximately stagnant fluid adjacent to the surface, and return. This fluid is assumed to be at $t_w$, and a convective Nusselt number of 2, between the gas and the particle, is assumed (*15*).
3. While the particle is at the surface, it also loses heat by conduction to a packet of particles of thickness $L$ situated between the wall particle and the bulk of the bed.

Other assumptions regarding radiation, thermal properties, etc., are as for model I. The basic channel for heat flow is, therefore, as illustrated in Figure 2.

Under these assumptions, the dimensionless differential equation and boundary conditions for the system are Equations (1), (2), (3), and

$$T_m(0, a) = T(a) \tag{21}$$

$$T(0) = 0 \tag{22}$$

$$\frac{dT}{da} = \gamma(1 - T) + \lambda \frac{\partial T_m}{\partial x}(0, a) \tag{23}$$

where

$$T(a) = \frac{t(a) - t_b}{t_w - t_b}$$

$$\lambda = \frac{12\ k_g}{k_m} \frac{\rho_m}{\rho_s} \tag{24}$$

$$\gamma = \frac{3}{2} \frac{\rho_m}{\rho_s}$$

and where $t(a)$ is the temperature of the surface particle, assumed uniform throughout the particle. Other quantities are as in model I. Equation (23) is the heat balance for the surface particle. This system of equations is similar to that of Ziegler et al. (*15*) but includes the additional heat loss from the surface particle to the bed. The model is the film penetration variant of the model presented briefly by Koppel et al. (*7*). It becomes identical to this latter model if Equation (3) is replaced by Equation (6).

Defining the instantaneous Nusselt number as before, and obtaining the instantaneous heat flux by considering a heat balance for the surface particles, we obtain

$$N_{Nu}(a) = 2\pi \frac{k_g}{k_m} \mu[1 - T(a)] \tag{25}$$

Applying the Laplace transformation to the model, we obtain

$$N_{Nu}(p) = 2\pi \frac{k_g}{k_m} \mu \frac{p + \gamma\sqrt{p} \coth (\sqrt{p}D_p/L)}{p[p + \lambda + \gamma\sqrt{p} \coth (\sqrt{p}D_p/L)]} \tag{26}$$

Inversion of Equation (26) is formidable but unnecessary for obtaining average coefficients by using a gamma residence time distribution (*7*).

#### Average Nusselt Number

For an exponential age density [Equation (11)], the average Nusselt number is obtained by using Equation (11) of Part I. After rearrangement, the result is

$$\eta_2(\zeta_2; \xi_2) = \frac{1}{1 + \zeta_2(\bar{\tau}, \xi_2)} \tag{27}$$

where

$$\eta_2 = \frac{\overline{N}_{Nu}}{2\pi\mu k_g/k_m}$$

$$\zeta_2 = \frac{\lambda\bar{\tau}}{1 + \gamma\sqrt{\bar{\tau}} \coth (\xi_2/\sqrt{\bar{\tau}})} \tag{28}$$

$$\xi_2 = L/D_p$$

This is the basic result of model II.

#### Asymptotic Values

As in model I, define the dimensionless contact coefficient as the instantaneous Nusselt number at zero age. Then, allowing $\bar{\tau} \to 0$ in Equation (27), we get

$$\eta_2(0; \xi_2) = 1 \tag{29}$$

which may be used to compute the contact coefficient for model II. This presents an alternative value to that of Baskakov. In the form of Equation (20), the result is

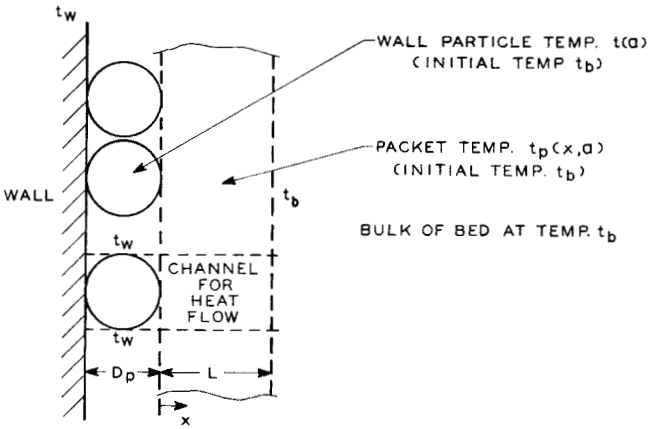


**Fig. 2. Geometry for model II.**

$$M = 2\pi\mu \frac{k_g}{k_m} \tag{30}$$

In all cases studied here, Equation (30) gave lower values of $M$ than did Equation (20). As $\bar{\tau} \to \infty$, we obtain from Equation (27)

$$\eta_2(\infty; \xi_2) = \frac{1}{1 + \xi_2\lambda/\gamma} \tag{31}$$

This may be used with an observed value of $h_{mf}$ to compute the parameter $\xi_2$. As in model I, physically correct forms of the limiting values are obtained. Operating on Equation (27), we obtain

$$\eta_2(\zeta_2; \infty) = \frac{1}{1 + \zeta_2(\bar{\tau}, \infty)} \tag{32}$$

where

$$\zeta_2(\bar{\tau}, \infty) = \frac{\lambda\bar{\tau}}{1 + \gamma\sqrt{\bar{\tau}}} \tag{33}$$

Equation (32) is analogous to Equation (16) and is the same as that used for the Ziegler model $\alpha = 0$ to obtain the computations in Table 1 of Part I (*7*).

## COMPARISON OF THEORY WITH DATA

Predicted transport coefficients from the theoretical models were compared with data obtained in a stirred fluidized bed. As pointed out earlier, this stirring ensured that no bubbles were present at the test surface. Residence time data were measured for the three sizes of glass. Residence times for the copper, aluminum, and alumina particles were estimated from the dimensionless plot of $\bar{\theta}\, v_{mf}/D_p$ vs. $v/v_{mf}$, obtained in Part III (*12*) by using the residence time data for the cellulose acetate and the glass particles. As a consequence, the comparisons of results for the metal and the alumina particles are less reliable, since they depend on the postulated $\bar{\theta}\, v_{mf}/D_p$ vs. $v/v_{mf}$ relationship. Packet properties were estimated in terms of particle properties by using methods presented by Mickley (*9*). These are given in Table 2. For model II, square packing of the particles at the surface ($\mu = 1$) was assumed. This conforms roughly with the type of packing observed at the bed wall.

#### Glass Data

In computing theoretical values from Equations (12) and (27), it was found that $\xi_1$ and $\xi_2$ were in all cases sufficiently large that the results were identical to those obtained from Equations (16) and (32), respectively. This

TABLE 2. PACKET THERMAL PROPERTIES*

| Particle type | Weight mean particle diam., ft. × $10^3$ | Density, $\rho m$, lb./cu. ft. | Packet properties, minimum fluidization: Conductivity, $k_m$, B.t.u./(hr.)(ft.)(°F.) | Specific heat, $c_m$, B.t.u./(lb.)(°F.) | Heat transfer coefficient, $h_{mf}$, B.t.u./(hr.)(sq. ft.)/(°F) |
|---|---|---|---|---|---|
| No. 1 glass | 2.65 | 92.0 | 0.105 | 0.17 | 8.5 |
| No. 2 glass | 1.94 | 91.0 | 0.105 | 0.17 | 6.4 |
| No. 3 glass | 1.03 | 91.0 | 0.103 | 0.17 | 3.7 |
| No. 1 copper | 2.00 | 331.6 | 0.31 | 0.10 | 17.3 |
| No. 2 copper | 1.05 | 325.5 | 0.31 | 0.10 | 9.4 |
| No. 1 alumina | 1.98 | 112.0 | 0.11 | 0.193 | 10.8 |
| No. 2 alumina | 0.99 | 115.0 | 0.11 | 0.193 | 5.4 |
| Aluminum | 0.98 | 93.6 | 0.25 | 0.224 | 7.2 |

* Estimated by methods presented by Mickley (9).

assertion will be graphically verified later. Therefore, these latter two equations, which have the common form

$$\eta = \frac{1}{1+\zeta} \tag{34}$$

were used to evaluate models I and II. Figure 3 is a plot of Equation (34) together with the data points. Excellent agreement is obtained with model I, the average absolute deviation of data from model I being 13%. For model II, the agreement is generally good, except at the low values of $\zeta$ which correspond to high velocities. Average absolute deviation from model II is 25%. The observed Nusselt numbers at low $\zeta$ are higher than the predicted dimensionless contact coefficient of Equation (30), indicating an inadequacy in this relation at high velocity. The assumption of spherically symmetric conduction from the stagnant gas to the wall particle (Nusselt number of 2 between gas and particle) may be particularly bad at high velocity. On the other hand, Baskakov's approach, which was used in model I in the form of Equation (20), apparently gives good values for the glass particles at all velocities studied here. In general, we conclude from Figure 3 that the postulated mechanisms and models are sound and that knowledge of the average residence time enables acceptably accurate estimation of the heat transfer coefficients in a fluidized bed.

Figure 4 is a plot of model I in the form of $\eta_1$ vs. $\zeta_1^2$. This latter quantity is $M^2\bar{\tau}$ and is, therefore, proportional to the mean residence time, while the ordinate reduces to $\bar{h}/h_c$ and is, therefore, proportional to the heat transfer coefficient. The glass data have been replotted onto Figure 4, along with data from the other systems to be discussed later. The theoretical curves for model I have been plotted for various values of the parameter $\xi$, by using Equation (12). Values of $\xi_1$ determined for each experimental system are given on Figure 4. From these values and the theoretical curves, one concludes that in all tests conducted here the film mechanism never became important. In other words, residence times were sufficiently short that the heat never penetrated to the characteristic length $L$. This explains why Equation (16), which does not require knowledge of the quantity $h_{mf}$, can be used as successfully, as indicated in Figure 3, to predict heat transfer coefficients. We therefore conclude that, for the system studied here, values of $h_{mf}$ are not required for prediction of $\bar{h}$ with model I. This conclusion may not be true for other systems, such as liquid fluidized beds.

Equation (17) is also plotted on Figure 4. This relation describes the theoretical predictions of model I when the dimensionless contact coefficient becomes infinite, or, what is equivalent, when the contact resistance is taken to be zero. (In addition, the parameter $\xi_1$ is taken to be infinite; this point will be discussed below.) Particularly for the smaller values of $\zeta_1$, the glass data clearly show that poor predictions result from the assumption of zero contact resistance. We conclude that the glass data verify the existence of a contact resistance. As $\zeta_1$ becomes large, Equations (16) and (17) converge. Physically, this occurs because as the residence time increases, the effective resistance of the packet becomes much larger than the contact resistance, owing to the absorption of heat, and the packet resistance controls the heat transfer process. Therefore, the predictions of Equations (16) and (17) are essentially identical for large $\zeta_1$. For finite values of the parameter $\xi_1$ but with zero contact resistance, Equation (18), the theoretical curves will be related to the curve for Equation (17) in much the same manner that the curves for Equation (12) are related to those for Equation (16). Since the predictions of Equation (17) are already too high, and since the values of $\xi_1$ corresponding to the data have already been shown to be effectively infinite, there is no point to plotting Equation (18) on Figure 4. The conclusion regarding the necessity of a nonzero contact resistance will remain unchanged.

An apparent anomaly exists in comparing the works of

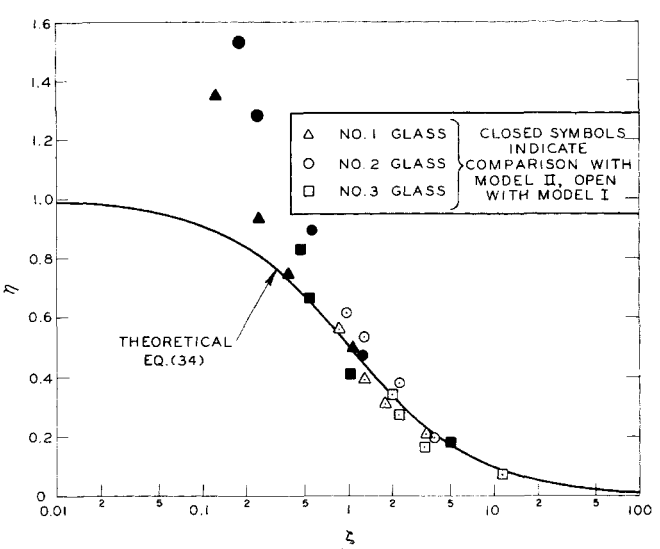


Fig. 3. Heat transfer data for glass particles compared with predictions from models I and II.

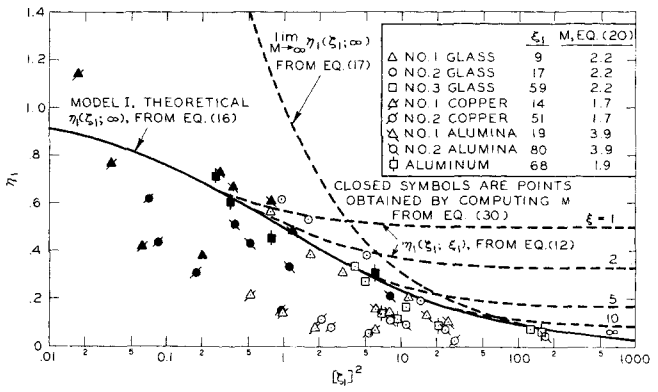


Fig. 4. Heat transfer data for all particles compared with predictions from model I.

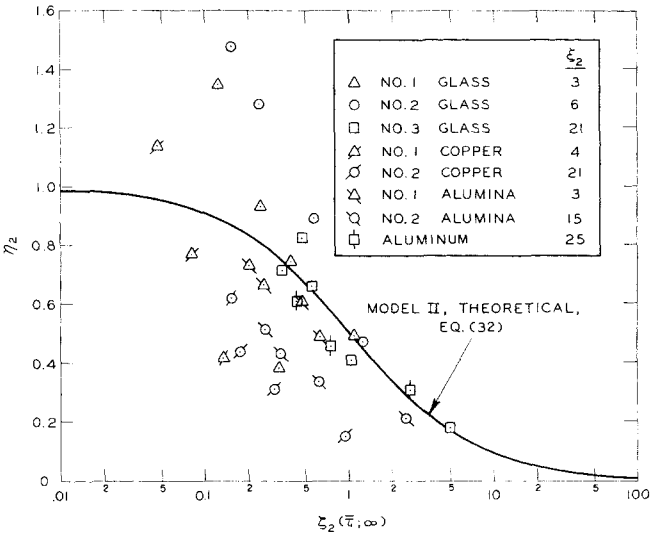


Fig. 5. Heat transfer data for all particles compared with predictions from model II.

Mickley (9) and Baskakov (2). The former used Equation (17) and the latter Equation (16), and both showed that they could predict heat transfer coefficients in good agreement with the same experimental data. The reason these authors obtained the same predictions using different equations is that they used different values for the average residence time or, equivalently, for renewal frequency. Two types of renewal frequency were observed by Mickley. They were determined by an examination of the temperature transience in a low heat capacity heater immersed in the bed. The first type of renewal frequency, which was the larger of the two, corresponded to changes in the sign of the derivative of the time-temperature curve for this heater. Mickley terms this the frequency of partial replacement of packets at the surface and postulates that it corresponds to the frequency of bubbles passing close to, but not touching, the heater surface. The second type of renewal frequency corresponded to very sharp changes in the temperature of the heater. These changes are assumed to be due to bubbles directly contacting, and removing all particles from, the surface. Mickley terms this renewal frequency the frequency of total replacement of packets at the surface.

Mickley uses the slower frequency of total replacement in his equation for the heat transfer coefficient, whereas Baskakov uses the faster partial replacement frequency. This shows why their predictions agree. Mickley's equation [Equation (17)] would normally predict higher coefficients (Figure 4), but by using lower frequencies and therefore longer residence times, he obtains coefficients which are close to those predicted by Baskakov, who used a contact resistance but shorter residence times [Figure 4, Equation (16)].

For the system used in the present work, there is clearly only one kind of replacement frequency, the frequency of packets traversing the heat transfer surface. No bubbles are present, so that there is no total replacement. This is a simpler system and therefore more easily understood. Figure 4, based on the only possible replacement frequency for the present system, demonstrates the necessity of including a contact resistance in the model to predict heat transfer coefficients for the gas fluidized beds studied here.

#### Data for Other Particles

Measured heat transfer coefficients for the copper, alumina, and aluminum particles are compared (along with the coefficients for the glass particles) with the theoretical predictions of model I in Figure 4 and with those of model II in Figure 5. The range of $v/v_{mf}$ was 1.0 to 1.8. The residence times were not actually measured for copper, alumina, and aluminum but were estimated from the postulated $\bar{\theta}\, v_{mf}/D_p$ vs. $v/v_{mf}$ relation presented in Part III (12).

In Figure 4, the open symbols show that the measured coefficients, particularly for the metal particles, copper and aluminum, are much lower than predictions from model I. Possible explanations for the poor predictions are that the mean residence times are in error and/or that the values of $M$ calculated from Equation (20) are incorrect. Assuming that the model is valid in general (which appears to be true in view of Figure 3), we may calculate the residence times which would produce agreement with the theoretical curves. This procedure results in dimensional residence times of the order of 50 to 100 sec. This is at variance with visual observations of the bed surface, which showed residence times to be of the order of a few seconds. It is therefore more likely that the values of $M$, obtained by using Baskakov's approach through Equation (20), are in error. Possibly, Baskakov's approach breaks down owing to the high $k_s$. The penetration of thermal gradients into the surface particles will be significant. On the other hand, the value of $M$ predicted by model II, Equation (30), considers primarily gas-phase resistance, thus producing a relating higher contact resistance (lower $M$) when the discrepancy between solid and gas conductivity is greater. The closed, or solid, symbols on Figure 4 show the comparison between theory and data for copper, alumina, and aluminum, when $M$ is computed from Equation (30). The improvement in the agreement, particularly for aluminum and No. 1 alumina, is clearly evident from this graphical comparison. A more quantitative description of the results obtained by using Equation (30) to compute $M$ is presented in Table 3.* For all particles except glass, the predictions are improved when Equation (30) is used; predictions have an overall average deviation of 24%.

Botterill (3) observed comparable results for copper particles; the predicted heat transfer coefficients from zero contact resistance are much higher than those measured. To account for this, he postulated a stagnant film of gas, of thickness 0.1 $D_p$, between the surface and particles. By using this approach, the value for No. 1 copper, for example, is $M = 0.5$, while Equations (30) and (20) yield 0.3 and 1.7, respectively.

* See footnote on p. 457.

Figure 5 shows that accuracy comparable to that of model I can be obtained for the copper, alumina, and aluminum particles when predictions are based on model II. Here again, predictions obtained by using Equation (27) with the values of $\xi_2$ presented on Figure 5 are negligibly different from those obtained by using $\xi_2 = \infty$, that is, by using Equation (32). Therefore, for all conditions studied in the present work, the value of $h_{mf}$ need not be known for prediction of $\overline{h}$.

When we consider the various assumptions made, especially with regard to estimation of residence times, Figures 4 and 5 show that both models are useful in predicting heat transfer coefficients, although the contact resistance of Baskakov cannot be used for high conductivity particles.

In general, if a smooth curve were drawn through the four points for each specific system, the slope would be of greater magnitude than that of the theoretical curve. This may be caused by a velocity effect. Decreasing $\zeta$ corresponds to increasing velocity, which increases the effective radial and axial diffusivities of the packets in contact with the surface and therefore increases the heat transfer coefficient. Such an effect is not accounted for in models I and II.

## CONCLUSIONS

Knowledge of average residence times and semitheoretical estimation of a contact resistance enables acceptable prediction of surface to bed heat transfer coefficients in stirred gas fluidized beds by using surface renewal models.

A dimensionless correlation of average residence times may be useful for estimation of heat transfer coefficients in particle systems for which direct residence time measurements are not available.

Heat transport from surfaces to the gas fluidized beds studied here is apparently a pure penetration type of process. Residence times are not sufficiently long to activate a film type of mechanism. This is not expected to be true for liquid fluidized beds.

Equation (12) is a generally useful transport model for surface renewal processes. It contains both a contact resistance and a film penetration mechanism and is easily specialized to previous models by appropriate limiting processes.

Further work is necessary to account for the effects of bubbles. Two sources of possible influence of bubbles on heat transfer coefficients are an increase in the coefficient caused by decreasing particle residence times, and a decrease in the coefficient caused by a decrease in effective solids density at the heater surface. Techniques for acceptably accurate determination of residence times and solids density, in the presence of bubbles, are required. The results of the present paper can then be applied directly to predict heat transfer coefficients.

## NOTATION

$a$ = dimensionless age
$D_p$ = particle diameter
$h$ = overall heat transfer coefficient
$\overline{h}$ = surface average heat transfer coefficient
$h_c$ = contact heat transfer coefficient
$k$ = thermal conductivity
$L$ = dimensional characteristic length
$M$ = contact Nusselt number
$N_{Nu}$ = Nusselt number
$p$ = Laplace transform variable
$q$ = heat flux
$q(a)$ = instantaneous heat flux from wall to bed
$t$ = dimensional temperature
$T$ = dimensionless temperature
$v$ = superficial gas velocity
$x$ = dimensionless distance
$y$ = dimensional distance

### Greek Letters

$\alpha$ = thermal diffusivity
$\gamma$ = factor in model II
$\zeta$ = residence time group, defined in Equations (13) and (32)
$\eta$ = heat transfer group, defined in Equations (13) and (32)
$\theta$ = dimensional time, dimensional residence time
$\lambda$ = factor in model II
$\mu$ = particle packing factor; $\mu/D_p^2$ = particles per unit area of the heated surface
$\xi$ = film thickness group, defined in Equations (13) and (32)
$\rho$ = density
$\tau$ = dimensionless residence time
$\phi$ = age density function

### Subscripts

$b$ = bulk of bed
$g$ = gas
$m$ = packet
$mf$ = minimum fluidization
$s$ = solid
$w$ = wall
1 = model I
2 = model II

### Superscripts

$-$ = mean value over distribution
$*$ = nondimensional quantity defined by using $L$ as the length parameter

## LITERATURE CITED


1. Baddour, R. F., and C. Y. Yoon, *Chem. Eng. Progr., Symposium Ser.*, No. 32, **57**, 35-50 (1961).
2. Baskakov, A. P., *Intern. Chem. Eng.*, **4**, 320-324 (1964).
3. Botterill, J. S. M., M. H. D. Butt, G. L. Cain, and K. A. Redish, paper presented at International Symposium on Fluidization, Eindhoven (June, 1967)
4. Botterill, J. S. M., K. A. Redish, D. K. Ross, and J. R. Williams, "Proceedings of Symposium on Interaction Between Fluids and Particles," pp. 183-189, London, England (1962).
5. Botterill, J. S. M., and J. R. Williams, *Trans. Inst. Chem. Engrs.*, **41**, 217-230 (1963).
6. Carslaw, H. S., and J. C. Jaeger, "Conduction of Heat in Solids," 2 ed., Oxford Univ. Press, London, England (1959).
7. Koppel, L. B., R. D. Patel, and J. T. Holmes, *AIChE J.*, **12**, 941-946 (1966).
8. *Ibid.*, 947-955.
9. Mickley, H. S., and D. F. Fairbanks, *ibid.*, **1**, 374-384 (1955).
10. ————, and R. D. Hawthorn, *Chem. Eng. Progr. Symposium Ser. No. 32*, **57**, 51-60 (1961).
11. Patel, R. D., Ph.D. thesis, Purdue Univ., Lafayette, Ind. (Aug., 1967).
12. ———, L. B. Koppel, and J. T. Holmes, *AIChE J.*, **16**, No. 3, p. 456 (May, 1970).
13. Ruckenstein, Eli, "Proceedings of the Third International Heat Transfer Conference," Vol. 4, pp. 298-301, Chicago, Ill. (1966).
14. Toor, H. L., and J. M. Marchello, *AIChE J.*, **4**, 97-101 (1958).
15. Ziegler, E. N., L. B. Koppel, and W. T. Brazelton, *Ind. Eng. Chem. Fundamentals*, **3**, 324-328 (1964).


*Manuscript received December 26, 1967; revision received November 7, 1968; paper accepted November 11, 1968.*